

Investigation of interaction of circularly and linearly polarized photon beams with polarized ^3He target

H. Witała^{1,*}, J. Golak¹, R. Skibiński¹, K. Topolnicki¹, and V. Urbanevych¹

¹*M. Smoluchowski Institute of Physics,
Jagiellonian University, PL-30348 Kraków, Poland*

(Dated: December 9, 2019)

arXiv:1912.03122v1 [nucl-th] 6 Dec 2019

Abstract

Photodisintegration of polarized ${}^3\text{He}$ by linearly or circularly polarized photons offers a rich choice of observables which can be calculated with high precision using a rigorous scheme of three-nucleon Faddeev equations. Using the (semi)phenomenological AV18 nucleon-nucleon potential combined with the Urbana IX three-nucleon force we investigate sensitivity of ${}^3\text{He}$ photodisintegration observables to underlying currents taken in the form of a single-nucleon current supplemented by two-body contributions for π - and ρ -meson exchanges or incorporated by the Siegert theorem. Promising observables to be measured for two- and three-body fragmentation of ${}^3\text{He}$ are identified. These observables form a challenging test ground for consistent forces and currents being under derivation within the framework of chiral perturbation theory. For three-body ${}^3\text{He}$ photodisintegration several kinematically complete configurations, including SST and FSI, are also discussed.

PACS numbers: 21.30.-x, 21.45.-v, 24.10.-i, 24.70.+s

I. INTRODUCTION

Application of effective field theoretical methods in the form of chiral perturbation theory (ChPT) puts investigation of properties of nuclear systems and their reactions on a new qualitative and quantitative level. Derivation of consistent two- and many-body internucleonic forces, and particularly the construction of nucleon-nucleon (NN) [1–5] and three-nucleon (3N) [6–8] interactions up to a fourth (N^4LO) order of the chiral expansion, provided a well grounded nuclear Hamiltonian, allowing for investigations of the importance of a three-nucleon force on a much more solid theoretical basis [9–12].

Progress in the development of numerical methods for nuclear structure calculations together with the availability of rigorous treatments of few-nucleon reactions within the Faddeev scheme made it possible to apply chiral two- and three-nucleon forces in nuclear structure and 3N reaction calculations, and, by comparison of theoretical predictions to data, to test the underlying dynamics. In this respect, the 3N system for which a large data base of high precision cross sections and spin observables is available ([13–23] and references

* henryk.witala@uj.edu.pl

therein) for elastic nucleon-deuteron (Nd) scattering and the deuteron breakup reaction is especially important.

For the electromagnetic sector an additional ingredient, the electromagnetic current has to be included. Investigations of its structure are less advanced due to experimental difficulties as well as due to the lack of a consistent treatment of forces and currents [24]. This situation has changed with the recent derivations of electro-weak currents within ChPT [25–30], which are, at least partly, consistent up to a given order of the chiral expansion to the corresponding chiral nuclear interaction ¹. With the advent of consistent forces and currents the number of reactions in which details of chiral dynamics can be studied will increase significantly. One of such reactions is photodisintegration of ³He which can lead to two- and three-body fragmentation in the final state. For energies of the incoming photons below the π -production threshold the Faddeev scheme allows one to get numerically exact predictions. This, together with the fact, that photodisintegration of ³He offers numerous observables, seems to predispose these reactions to become a valuable tool to test the dynamics with its electromagnetic current operator ingredient.

With the availability of low energy high intensity polarized photon beams [31, 32] and polarized ³He targets [33, 34] a set of observables offered by two- and three-body photodisintegration of ³He, which could be measured with sufficient precision, is substantially extended and includes, in addition to the unpolarized cross section, also analyzing powers and spin correlation coefficients.

It is the aim of the present study to investigate the sensitivity of observables in low energy $\vec{\gamma} + {}^3\bar{H}e$ photodisintegration to underlying currents. In anticipation of application of consistent chiral interactions and currents we use the (semi)phenomenological AV18 [35] nucleon-nucleon potential combined with the Urbana IX [36] three-nucleon force and the current operator taken in the form of a single nucleon current supplemented by two-body contributions either in the form of explicit π - and ρ -meson exchanges or incorporated by the Siegert theorem [37]. We solve the 3N Faddeev equations for ³He photodisintegration [37] with such dynamics and calculate all possible observables for two- and three-body fragmentation of polarized ³He induced with linearly or circularly polarized photons, investigating their sensitivity to the underlying current.

¹ Note that despite the fact that the operator form of chiral currents is known at the lowest orders, applications of chiral many-nucleon forces and currents in practical 3N calculations is presently questionable due to the lack of their consistent regularization.

The paper is organized as follows: in Sec. II we briefly describe the theoretical formalism and derive expressions for polarization observables in ${}^3\text{He}$ photodisintegration induced by circularly or linearly polarized photons interacting with a polarized ${}^3\text{He}$. We present and discuss results for two- and three-body fragmentation of ${}^3\text{He}$ in Sec. III and summarize and conclude in Sec. IV.

II. THEORETICAL FORMALISM

In the following we present briefly our treatment of ${}^3\text{He}$ photodisintegration within the Faddeev scheme. For details of the theoretical formalism and numerical performance we refer the reader to [37, 38].

The basic quantities from which all observables for photodisintegration of ${}^3\text{He}$ can be calculated are the nuclear matrix elements $N_{\{\mu_i\}}^{\lambda m}$ [37]:

$$N_{\{\mu_i\}}^{\lambda m} \equiv \langle \Psi_{f,\{\mu_i\}}^{(-)} | \vec{j}_\lambda | \Psi_m^{3He} \rangle \quad (1)$$

of the ${}^3\text{He}$ current operator \vec{j}_λ ($\lambda = \pm 1$) between the initial ${}^3\text{He}$ state $|\Psi_m^{3He}\rangle$ with the spin projection m onto the z-axis defined by the momentum of the incoming photon, and the final 3N scattering state $|\Psi_{f,\{\mu_i\}}^{(-)}\rangle$, which is either two-body proton-deuteron (pd) or three-body proton-proton-neutron (ppn) fragmentation, with corresponding spin projections of the outgoing particles $\{\mu_i\}$.

Assuming that three nucleons interact with two- and three-nucleon forces, and writing down 3N Faddeev equations for the Faddeev components of 3N scattering states, allows us to express the nuclear matrix elements for two- and three-body fragmentation of ${}^3\text{He}$ in terms of an auxiliary state $|\tilde{U}\rangle$, which fulfills the following Faddeev-like equation [37]:

$$\begin{aligned} |\tilde{U}\rangle = & [tG_0 + \frac{1}{2}(1+P)V^{(1)}G_0(1+tG_0)](1+P)\vec{j}_\lambda|\Psi_m^{3He}\rangle \\ & + [tG_0P + \frac{1}{2}(1+P)V^{(1)}G_0(1+tG_0)P]|\tilde{U}\rangle . \end{aligned} \quad (2)$$

The permutation operator $P \equiv P_{12}P_{23} + P_{13}P_{23}$ is given by interchanges P_{ij} of nucleons i and j and the NN t-operator t results from the employed NN potential through the two-body Lippmann-Schwinger equation. $V^{(1)}$ is a part of a 3N force operator $V_{123} = V^{(1)} + V^{(2)} + V^{(3)}$, which is symmetrical under exchange of nucleons 2 and 3.

Using the state $|\tilde{U}\rangle$ the nuclear matrix element for pd fragmentation of ${}^3\text{He}$ is given by [37]:

$$N_{\mu_p\mu_d}^{\lambda m} = \langle \phi_q | (1 + P) \vec{j}_\lambda | \Psi_m^{3\text{He}} \rangle + \langle \phi_q | P | \tilde{U} \rangle, \quad (3)$$

with $|\phi_q\rangle \equiv |\varphi_d \mu_d \mu_p\rangle$, where $|\varphi_d\rangle$ is the internal deuteron state, μ_d and μ_p are the deuteron and proton spin projections, respectively, and \vec{q}_p is a relative proton-deuteron momentum.

For three-body breakup the nuclear matrix element is given by [37]:

$$N_{\mu_1\mu_2\mu_3}^{\lambda m} = \langle \varphi_0 | (1 + tG_0)(1 + P) \vec{j}_\lambda | \Psi_m^{3\text{He}} \rangle + \langle \varphi_0 | (1 + tG_0)P | \tilde{U} \rangle, \quad (4)$$

with $|\varphi_0\rangle \equiv (1 - P_{23})|\vec{p}\mu_2\mu_3\rangle$, where μ_i ($i = 1, 2, 3$) are nucleons' spin projections, and \vec{p} , \vec{q} are standard Jacobi momenta.

The density matrix of polarized photons written in the spherical basis (rows labelled with $\lambda = +1$ and -1) is given by [39]:

$$\rho^\gamma = \frac{1}{2} \begin{pmatrix} 1 + P_c^\gamma & P_x^\gamma + iP_y^\gamma \\ P_x^\gamma - iP_y^\gamma & 1 - P_c^\gamma \end{pmatrix} \quad (5)$$

where P_x^γ (P_y^γ) is a linear and P_c^γ a circular polarization of photon.

The density matrix of polarized ${}^3\text{He}$ (rows labelled with the ${}^3\text{He}$ spin projection $m = +\frac{1}{2}$ and $m = -\frac{1}{2}$), with a polarization vector $\vec{P} = (P_x, P_y, P_z)$ is given by:

$$\rho^{3\text{He}} = \frac{1}{2} \begin{pmatrix} 1 + P_z & P_x + iP_y \\ P_x - iP_y & 1 - P_z \end{pmatrix} \quad (6)$$

For the initial channel $\vec{\gamma} + {}^3\vec{H}e$ with the z-axis taken in the direction of the incoming photon beam, the incoming state density matrix is a direct product of the photon and ${}^3\text{He}$ density matrices:

$$\rho^{in} = \rho^\gamma \otimes \rho^{3\text{He}} = \frac{1}{4} \begin{pmatrix} 1 + P_c^\gamma & P_x^\gamma + iP_y^\gamma \\ P_x^\gamma - iP_y^\gamma & 1 - P_c^\gamma \end{pmatrix} \otimes \begin{pmatrix} 1 + P_z & P_x + iP_y \\ P_x - iP_y & 1 - P_z \end{pmatrix} \quad (7)$$

The cross section with polarized photons and polarized ${}^3\text{He}$: $\sigma^{pol} = Tr(N\rho^{in}N^+)$, with the full transition amplitude N containing the nuclear matrix elements $N_{\{\mu_i\}}^{\lambda m}$, is given by:

$$\begin{aligned} \sigma^{pol} = & \sigma^o (1 + P_c^\gamma A_c^\gamma + P_x^\gamma A_x^\gamma + P_y^\gamma A_y^\gamma + P_x A_x^{3\text{He}} + P_y A_y^{3\text{He}} + P_z A_z^{3\text{He}} \\ & + P_c^\gamma P_z C_{c,z}^{\gamma,3\text{He}} + P_c^\gamma P_x C_{c,x}^{\gamma,3\text{He}} + P_c^\gamma P_y C_{c,y}^{\gamma,3\text{He}} + P_x^\gamma P_z C_{x,z}^{\gamma,3\text{He}} + P_x^\gamma P_x C_{x,x}^{\gamma,3\text{He}} \end{aligned}$$

$$+ P_x^\gamma P_y C_{x,y}^{\gamma, {}^3\text{He}} + P_y^\gamma P_z C_{y,z}^{\gamma, {}^3\text{He}} + P_y^\gamma P_x C_{y,x}^{\gamma, {}^3\text{He}} + P_y^\gamma P_y C_{y,y}^{\gamma, {}^3\text{He}}) \quad (8)$$

with photon analyzing powers: A_c^γ , A_x^γ , and A_y^γ , ${}^3\text{He}$ -analyzing powers: $A_x^{3\text{He}}$, $A_y^{3\text{He}}$, and $A_z^{3\text{He}}$, and spin correlation coefficients: $C_{c,x}^{\gamma, {}^3\text{He}}$, $C_{c,y}^{\gamma, {}^3\text{He}}$, $C_{c,z}^{\gamma, {}^3\text{He}}$, $C_{x,x}^{\gamma, {}^3\text{He}}$, $C_{x,y}^{\gamma, {}^3\text{He}}$, $C_{x,z}^{\gamma, {}^3\text{He}}$, $C_{y,x}^{\gamma, {}^3\text{He}}$, $C_{y,y}^{\gamma, {}^3\text{He}}$, and $C_{y,z}^{\gamma, {}^3\text{He}}$ given by:

$$\begin{aligned}
A_c^\gamma &= \frac{\sum_{\{\mu_i\}m} N_{\{\mu_i\}}^{+1m} N_{\{\mu_i\}}^{*+1m} - N_{\{\mu_i\}}^{-1m} N_{\{\mu_i\}}^{*-1m}}{\sum_{\{\mu_i\}m\lambda} |N_{\{\mu_i\}}^{\lambda m}|^2} \\
A_x^\gamma &= \frac{\sum_{\{\mu_i\}m} N_{\{\mu_i\}}^{+1m} N_{\{\mu_i\}}^{*-1m} + N_{\{\mu_i\}}^{-1m} N_{\{\mu_i\}}^{*+1m}}{\sum_{\{\mu_i\}m\lambda} |N_{\{\mu_i\}}^{\lambda m}|^2} = \frac{\sum_{\{\mu_i\}m} 2\Re \left[N_{\{\mu_i\}}^{+1m} N_{\{\mu_i\}}^{*-1m} \right]}{\sum_{\{\mu_i\}m\lambda} |N_{\{\mu_i\}}^{\lambda m}|^2} \\
A_y^\gamma &= \frac{\sum_{\{\mu_i\}m} i N_{\{\mu_i\}}^{+1m} N_{\{\mu_i\}}^{*-1m} - i N_{\{\mu_i\}}^{-1m} N_{\{\mu_i\}}^{*+1m}}{\sum_{\{\mu_i\}m\lambda} |N_{\{\mu_i\}}^{\lambda m}|^2} = \frac{\sum_{\{\mu_i\}m} -2\Im \left[N_{\{\mu_i\}}^{+1m} N_{\{\mu_i\}}^{*-1m} \right]}{\sum_{\{\mu_i\}m\lambda} |N_{\{\mu_i\}}^{\lambda m}|^2} \\
A_z^{3\text{He}} &= \frac{\sum_{\{\mu_i\}\lambda} N_{\{\mu_i\}}^{\lambda \frac{1}{2}} N_{\{\mu_i\}}^{*\lambda \frac{1}{2}} - N_{\{\mu_i\}}^{\lambda - \frac{1}{2}} N_{\{\mu_i\}}^{*\lambda - \frac{1}{2}}}{\sum_{\{\mu_i\}m\lambda} |N_{\{\mu_i\}}^{\lambda m}|^2} \\
A_x^{3\text{He}} &= \frac{\sum_{\{\mu_i\}\lambda} N_{\{\mu_i\}}^{\lambda \frac{1}{2}} N_{\{\mu_i\}}^{*\lambda - \frac{1}{2}} + N_{\{\mu_i\}}^{\lambda - \frac{1}{2}} N_{\{\mu_i\}}^{*\lambda \frac{1}{2}}}{\sum_{\{\mu_i\}m\lambda} |N_{\{\mu_i\}}^{\lambda m}|^2} = \frac{\sum_{\{\mu_i\}\lambda} 2\Re \left[N_{\{\mu_i\}}^{\lambda \frac{1}{2}} N_{\{\mu_i\}}^{*\lambda - \frac{1}{2}} \right]}{\sum_{\{\mu_i\}m\lambda} |N_{\{\mu_i\}}^{\lambda m}|^2} \\
A_y^{3\text{He}} &= \frac{\sum_{\{\mu_i\}\lambda} i N_{\{\mu_i\}}^{\lambda \frac{1}{2}} N_{\{\mu_i\}}^{*\lambda - \frac{1}{2}} - i N_{\{\mu_i\}}^{\lambda - \frac{1}{2}} N_{\{\mu_i\}}^{*\lambda \frac{1}{2}}}{\sum_{\{\mu_i\}m\lambda} |N_{\{\mu_i\}}^{\lambda m}|^2} = \frac{\sum_{\{\mu_i\}\lambda} -2\Im \left[N_{\{\mu_i\}}^{\lambda \frac{1}{2}} N_{\{\mu_i\}}^{*\lambda - \frac{1}{2}} \right]}{\sum_{\{\mu_i\}m\lambda} |N_{\{\mu_i\}}^{\lambda m}|^2} \\
C_{c,z}^{\gamma, {}^3\text{He}} &= \frac{\sum_{\{\mu_i\}} N_{\{\mu_i\}}^{+1\frac{1}{2}} N_{\{\mu_i\}}^{*+1\frac{1}{2}} + N_{\{\mu_i\}}^{-1-\frac{1}{2}} N_{\{\mu_i\}}^{*-1-\frac{1}{2}} - N_{\{\mu_i\}}^{+1-\frac{1}{2}} N_{\{\mu_i\}}^{*+1-\frac{1}{2}} - N_{\{\mu_i\}}^{-1\frac{1}{2}} N_{\{\mu_i\}}^{*-1\frac{1}{2}}}{\sum_{\{\mu_i\}m\lambda} |N_{\{\mu_i\}}^{\lambda m}|^2} \\
C_{c,x}^{\gamma, {}^3\text{He}} &= \frac{\sum_{\{\mu_i\}} N_{\{\mu_i\}}^{+1\frac{1}{2}} N_{\{\mu_i\}}^{*+1-\frac{1}{2}} + N_{\{\mu_i\}}^{+1-\frac{1}{2}} N_{\{\mu_i\}}^{*+1\frac{1}{2}} - N_{\{\mu_i\}}^{-1\frac{1}{2}} N_{\{\mu_i\}}^{*-1-\frac{1}{2}} - N_{\{\mu_i\}}^{-1-\frac{1}{2}} N_{\{\mu_i\}}^{*-1\frac{1}{2}}}{\sum_{\{\mu_i\}m\lambda} |N_{\{\mu_i\}}^{\lambda m}|^2} \\
&= \frac{\sum_{\{\mu_i\}} 2\Re \left[N_{\{\mu_i\}}^{+1\frac{1}{2}} N_{\{\mu_i\}}^{*+1-\frac{1}{2}} - N_{\{\mu_i\}}^{-1\frac{1}{2}} N_{\{\mu_i\}}^{*-1-\frac{1}{2}} \right]}{\sum_{\{\mu_i\}m\lambda} |N_{\{\mu_i\}}^{\lambda m}|^2} \\
C_{c,y}^{\gamma, {}^3\text{He}} &= \frac{\sum_{\{\mu_i\}} i N_{\{\mu_i\}}^{+1\frac{1}{2}} N_{\{\mu_i\}}^{*+1-\frac{1}{2}} + i N_{\{\mu_i\}}^{-1-\frac{1}{2}} N_{\{\mu_i\}}^{*-1\frac{1}{2}} - i N_{\{\mu_i\}}^{+1-\frac{1}{2}} N_{\{\mu_i\}}^{*+1\frac{1}{2}} - i N_{\{\mu_i\}}^{-1\frac{1}{2}} N_{\{\mu_i\}}^{*-1-\frac{1}{2}}}{\sum_{\{\mu_i\}m\lambda} |N_{\{\mu_i\}}^{\lambda m}|^2}
\end{aligned}$$

$$\begin{aligned}
C_{y,y}^{\gamma,{}^3\text{He}} &= \frac{\sum_{\{\mu_i\}} -N_{\{\mu_i\}}^{+1\frac{1}{2}} N_{\{\mu_i\}}^{*-1-\frac{1}{2}} + N_{\{\mu_i\}}^{+1-\frac{1}{2}} N_{\{\mu_i\}}^{*-1\frac{1}{2}} + N_{\{\mu_i\}}^{-1\frac{1}{2}} N_{\{\mu_i\}}^{*+1-\frac{1}{2}} - N_{\{\mu_i\}}^{-1-\frac{1}{2}} N_{\{\mu_i\}}^{*+1\frac{1}{2}}}{\sum_{\{\mu_i\}m\lambda} |N_{\{\mu_i\}}^{\lambda m}|^2} \\
&= \frac{\sum_{\{\mu_i\}} 2\Re \left[-N_{\{\mu_i\}}^{+1\frac{1}{2}} N_{\{\mu_i\}}^{*-1-\frac{1}{2}} + N_{\{\mu_i\}}^{+1-\frac{1}{2}} N_{\{\mu_i\}}^{*-1\frac{1}{2}} \right]}{\sum_{\{\mu_i\}m\lambda} |N_{\{\mu_i\}}^{\lambda m}|^2} \tag{9}
\end{aligned}$$

Some of these observables vanish for two- as well as for three-body in plane photodisintegration of ${}^3\text{He}$. Namely, assuming that outgoing particles move in a plane, which contains also the photon beam incoming along z-axis, leads to the following symmetry relation for the nuclear matrix elements $N_{\{\mu_i\}}^{\lambda m}$:

$$N_{\{-\mu_i\}}^{-\lambda-m} = (-1)^{(1-m-\lambda+\sum\mu_i)} N_{\{\mu_i\}}^{\lambda m} . \tag{10}$$

Applying that relation to the polarization observables of Eq. (9) shows, that the only nonvanishing analyzing powers are A_x^γ and $A_y^{3\text{He}}$, and the nonvanishing spin correlation coefficients are: $C_{c,z}^{\gamma,{}^3\text{He}}$, $C_{c,x}^{\gamma,{}^3\text{He}}$, $C_{x,y}^{\gamma,{}^3\text{He}}$, $C_{y,z}^{\gamma,{}^3\text{He}}$, and $C_{y,x}^{\gamma,{}^3\text{He}}$. The analyzing powers: A_c^γ , A_y^γ , $A_x^{3\text{He}}$, and $A_z^{3\text{He}}$, as well as spin correlation coefficients: $C_{c,y}^{\gamma,{}^3\text{He}}$, $C_{x,z}^{\gamma,{}^3\text{He}}$, $C_{x,x}^{\gamma,{}^3\text{He}}$, and $C_{y,y}^{\gamma,{}^3\text{He}}$, vanish.

The same is true for kinematically incomplete three-body fragmentation with a reaction plane formed by the incoming photon beam and the momentum of the one nucleon detected in the final state.

III. RESULTS AND DISCUSSION

To investigate the sensitivity of low energy ${}^3\text{He}$ photodisintegration observables to the underlying current operator we solved Faddeev-like Eq. (2) for the state $|\tilde{U}\rangle$ at three energies of the incoming photons: $E_\gamma = 15, 20, \text{ and } 30$ MeV, using our standard approach based on momentum space partial wave decomposition [13, 37, 40, 41]. The high precision (semi)phenomenological nucleon-nucleon potential AV18 [35] together with the Urbana IX [36] three-nucleon force was used. Including this 3N force reproduces the experimental ${}^3\text{He}$ binding energy. The AV18 potential contains electromagnetic parts [35]. They are all kept in our treatment of the ${}^3\text{He}$ bound state [42] but for the 3N continuum we keep only the strong forces. We solve the set of coupled integral equations in the two Jacobi variables by iteration, generating the multiple scattering series separately for each fixed total 3N system angular momentum J and parity. We neglect the coupling of states with total isospin $T = \frac{1}{2}$ and

$T = \frac{3}{2}$, which is due to charge independence breaking for neutron-proton (np) and proton-proton (pp) forces but keep both isospins T. The difference between pp and np forces is, however, taken into account by applying the “ $\frac{2}{3} - \frac{1}{3}$ ” rule [43, 44].

The single nucleon current was augmented by explicit π - and ρ -like two-body currents which fulfill the current continuity equation together with the corresponding parts of the AV18 potential [37]. As an alternative to explicit two-body contributions we employed the Siegert theorem [37], which induces many-body contributions to the current operator.

In Figs. 1-3 we show results for two-body photodisintegration of ${}^3\text{He}$. As shown in the previous section, from the set of 15 possible polarization observables for $\vec{\gamma} + {}^3\vec{H}e \rightarrow p + d$ process given by Eq. (9) only two analyzing powers: A_x^γ and A_y^{3He} , as well as 5 spin correlation coefficients: $C_{c,z}^{\gamma,3He}$, $C_{c,x}^{\gamma,3He}$, $C_{x,y}^{\gamma,3He}$, $C_{y,z}^{\gamma,3He}$, and $C_{y,x}^{\gamma,3He}$, do not vanish. Two observables, namely the unpolarized cross section $\frac{d\sigma}{d\Omega}$ and photon analyzing power A_x^γ show only small sensitivity to the treatment of the two-body contributions to the current operator, and predictions obtained with meson exchanges and Siegert theorem are close to each other. Changing the photon energy from $E_\gamma = 15$ MeV to 30 MeV diminishes the cross section by a factor of ≈ 3 . The analyzing power A_x^γ is, especially at the lower energy $E_\gamma = 15$ MeV, large and approaches a value close to 1 in a wide range of proton angles. The ${}^3\text{He}$ analyzing power A_y^{3He} reaches at $E_\gamma = 30$ MeV the value of ≈ 0.2 and reveals at both energies a similar and large sensitivity to the current operator.

Among the five nonvanishing spin correlation coefficients (see Figs. 2 and 3) $C_{y,z}^{\gamma,3He}$ is small and shows only moderate sensitivity to the current operator. The spin correlation $C_{c,z}^{\gamma,3He}$ (Fig. 2) at 15 MeV takes large values only at very forward and backward angles, being otherwise small. With increasing energy its sensitivity to the current grows. Spin correlations $C_{c,x}^{\gamma,3He}$, $C_{x,y}^{\gamma,3He}$, and $C_{y,x}^{\gamma,3He}$ behave similarly, being comparable in magnitude and showing quite large sensitivity to the underlying current.

For semi-inclusive 3-body photodisintegration ${}^3\vec{H}e(\vec{\gamma},p)np$ the set of nonvanishing spin observables is the same as for the two-body fragmentation. We show them in Figs. 4-6 together with the unpolarized cross section as a function of the outgoing laboratory energy of the detected proton at a laboratory proton angle $\theta_p = 30^\circ$. The unpolarized cross section $\frac{d^3\sigma}{d\Omega_p dE_p}$ shows a characteristic peak at the maximum energy of the outgoing proton caused by a final state interaction in the state 1S_0 of the undetected proton-neutron pair. The cross section drops with increasing photon energy, being reduced by a factor of ≈ 4 when

changing the photon energy from 15 to 30 MeV. The unpolarized cross section and the photon analyzing power A_x^γ shows only small sensitivity to the current, contrary to the spin correlation coefficients, which exhibit, with exceptions of $C_{x,y}^{\gamma,^3\text{He}}$ and $C_{y,x}^{\gamma,^3\text{He}}$ at $E_\gamma=15$ MeV, quite large differences along the outgoing proton energy when changing the type of two-body contributions to the current operator. For most of the presented observables that sensitivity seems to be similar at both photons energies.

Three-body fragmentation of ^3He caused by the interaction with incoming photon offers a unique possibility to reach a specific kinematically complete geometries of three outgoing nucleons identical to those populated in a kinematically complete nucleon-deuteron (Nd) breakup. Comparison of data in such kinematically complete configurations, reached either by pure hadronic interactions in Nd breakup or by electromagnetic and hadronic interactions in three-body fragmentation of ^3He , would be very interesting due to unresolved problems found for some kinematically complete measurements e.g. in the symmetric space-star (SST) geometry [45]. Data for such geometries gained from complimentary Nd and three-body ^3He photodisintegration and their comparison to theory could shed some light on the existing discrepancies. In Tab. I we compare the incoming photon laboratory energy E_γ of the ^3He photodisintegration with the laboratory kinetic energy E^{lab} of the incoming nucleon in the corresponding proton-induced deuteron breakup reaction, both processes having the same 3N system center-of-mass kinetic energy $E^{c.m.}$.

The kinematically complete geometries of three outgoing nucleons can be defined for three-body photodisintegration of ^3He analogously to their Nd breakup counterparts. For example for the final state configuration (FSI) the condition is the equality of momenta of two interacting nucleons in the final scattering state. For the SST three outgoing nucleons must move in their c.m. system with equal momentum magnitudes in a plane perpendicular to the incoming photon momentum and the relative angle between momenta is 120° like in the “Mercedes star” logo.

In the case of the final state interaction the condition of momentum equality of two nucleons permits finding, at each laboratory direction of outgoing nucleon, such a FSI geometry in which one from remaining two nucleons have the same momentum. In Figs. 7-9 we show nonvanishing observables for exclusive three-body photodisintegration of ^3He : $^3\vec{H}e(\vec{\gamma}, pp)n$, leading to a kinematically complete final state interaction configuration in which nucleons 1 and 3 (in this case proton and neutron, respectively) have the same momenta $\vec{p}_1 = \vec{p}_3$.

E_γ [MeV]	$E^{c.m.}$ [MeV]	E^{lab} [MeV]	p^{lab} [MeV/c]
15.0	7.2	14.2	164.2
20.0	12.2	21.7	203.2
30.0	22.1	36.7	265.2

TABLE I. The initial photon laboratory energy E_γ , the consequent center-of-mass kinetic energy of the ppn system $E^{c.m.}$ and the incident proton laboratory kinetic energy E^{lab} together with its momentum p^{lab} for the corresponding proton-induced deuteron breakup reaction with the same $E^{c.m.}$.

The observables are shown as a function of a production angle $\theta_1^{lab} = \theta_3^{lab}$ of such a FSI(1-3) configuration. The unpolarized cross section $\frac{d^5\sigma}{d\Omega_1 d\Omega_2 dS}$ shown in Fig. 7 reaches largest values for FSI(1-3) configurations produced at angles around $\theta_1^{lab} \approx 100^\circ$. Similarly to inclusive breakup, increasing the photon energy from 15 to 30 MeV diminishes the cross section by a factor of ≈ 2 . The FSI cross section at both energies is quite sensitive to the underlying current.

The FSI analyzing powers A_x^γ and A_y^{3He} show some slight sensitivity to the current operator only at the higher energy $E_\gamma = 30$ MeV. Interestingly enough, they are quite large in a wide range of FSI production angles.

FSI spin correlation coefficients offer more sensitivity to the current, particularly $C_{c,z}^{\gamma,3He}$ at $E_\gamma = 30$ MeV and $C_{c,x}^{\gamma,3He}$ at both energies. Also FSI spin correlation coefficients take large values in quite large regions of the FSI production angles.

Among numerous kinematically complete configurations of the Nd breakup reaction the SST configuration has attracted a special attention. The cross section for that geometry is very stable with respect to the underlying dynamics and dominated by the S-waves [45]. At low energies theoretical predictions deviate significantly from the available SST data [46–48]. The possibility to reach that geometry through ^3He three-body photodisintegration $^3\text{He}(\gamma,pp)n$ would help to shed some light on this problem.

In Fig. 10 we show the SST cross section $\frac{d^5\sigma}{d\Omega_1 d\Omega_2 dS}$ at three incoming photon energies $E_\gamma = 15, 20,$ and 30 MeV as a function of an arc-length of the S-curve. This curve, in the plane determined by the laboratory energies of two detected protons $E_1 - E_2$, contains all the kinematically allowed events. The SST condition is exactly fulfilled at a central part

of the S-curve at each photon energy. The SST cross section observed along the S-curve reveals only a weak sensitivity to the underlying current and the cross section drops quite rapidly with increasing photon energy, changing from $\frac{d^5\sigma}{d\Omega_1 d\Omega_2 dS} \approx 2 \frac{mb}{sr^2 MeV}$ at $E_\gamma = 15$ MeV to $\frac{d^5\sigma}{d\Omega_1 d\Omega_2 dS} \approx 0.3 \frac{mb}{sr^2 MeV}$ at $E_\gamma = 30$ MeV.

IV. SUMMARY AND CONCLUSIONS

Recent advances in high intensity polarized photon beams and polarized ^3He targets increased the number of observables to be measured in two- and three-body photodisintegration of ^3He . In addition to the unpolarized cross section also measurements of photon and ^3He analyzing powers as well as spin correlation coefficients are feasible. That possibility together with promising results achieved in derivation, in the framework of chiral perturbation theory, of consistent two- and three-nucleon forces as well as electro-weak currents, allows for comprehensive testing the chiral dynamics not only in pure hadronic systems but also in processes induced by the interaction of external electro-weak probes with nuclear systems.

Photodisintegration of polarized ^3He by polarized photon not only provides a rich choice of observables to be measured but, due to the availability of rigorous Faddeev techniques for solving the corresponding equations, allows one to compare such data with exact theoretical predictions for spin-dependent observables, thus extending the testing ground for nuclear dynamics.

We investigated the observables in two- and three-body fragmentation of ^3He with respect to their sensitivity to the underlying current by comparing results with two different treatments of two-body contributions, namely by taking them as direct meson exchanges or treating them by using Siegert theorem.

For two-body fragmentation we found that the unpolarized cross section and the photon analyzing power A_x^γ are practically insensitive to the underlying current. Large values of A_x^γ point to the feasibility of its measurement. Both these observables would be valuable for future testing of chiral dynamics. The sensitivity to the current operator of the ^3He analyzing power $A_y^{^3He}$ and the spin correlation coefficients predisposes them to test the current operator.

For semi-inclusive three-body fragmentation we found a similar behavior. While the unpolarized cross section and photon analyzing power A_x^γ show only a slight sensitivity to

the current, the ${}^3\text{He}$ analyzing power and spin correlation coefficients reveal sensitivity to the current practically at all the energies of the detected nucleon.

From the rich phase-space of the exclusive three-body ${}^3\text{He}$ fragmentation we investigated only the geometry of the final-state interaction and the symmetric space-star configuration. For FSI we found a sensitivity of the cross section to the underlying current while the analyzing powers show only very slight sensitivity. Among spin correlation coefficients the largest sensitivity is visible in $C_{c,x}^{\gamma,{}^3\text{He}}$. The sensitivity of the unpolarized SST cross section to the underlying current gets reduced with the increasing photon energy.

Summarizing, measurements of ${}^3\vec{H}e + \vec{\gamma}$ observables for both two- and three-body ${}^3\text{He}$ fragmentation seem feasible and such data would provide a valuable test for our understanding of electromagnetic processes, especially in the context of expected results based on chiral dynamics. We hope this work will guide preparations of new generation precise experiments on ${}^3\text{He}$ photodisintegration.

ACKNOWLEDGMENTS

This study has been performed within Low Energy Nuclear Physics International Collaboration (LENPIC) project and was supported by the Polish National Science Center under Grants No. 2016/22/M/ST2/00173 and 2016/21/D/ST2/01120. The numerical calculations were performed on the supercomputer cluster of the JSC, Jülich, Germany.

-
- [1] E. Epelbaum, W. Glöckle, and U.-G. Meißner, Nucl. Phys. **A747**, 362 (2005).
 - [2] E. Epelbaum, Prog. Part. Nucl. Phys. **57**, 654 (2006).
 - [3] R. Machleidt, D. R. Entem, Phys. Rep. **503**, 1 (2011).
 - [4] E. Epelbaum, H. Krebs, and U.-G. Meißner, Eur. Phys. J. A **51**, no. 5, 53 (2015).
 - [5] E. Epelbaum, H. Krebs, and U.-G. Meißner, Phys. Rev. Lett. **115**, 122301 (2015).
 - [6] E. Epelbaum *et al.*, Phys. Rev. C **66**, 064001 (2002).
 - [7] V. Bernard, E. Epelbaum, H. Krebs, and U.-G. Meißner, Phys. Rev. C **77**, 064004 (2008).
 - [8] V. Bernard, E. Epelbaum, H. Krebs, and U.-G. Meißner, Phys. Rev. C **84**, 054001 (2011).
 - [9] S. Binder *et al.* [LENPIC Collaboration], Phys. Rev. C **93**, 044002 (2016).

- [10] S. Binder *et al.* [LENPIC Collaboration], Phys. Rev. **C98**, 014002 (2018).
- [11] E. Epelbaum *et al.* [LENPIC Collaboration], Phys. Rev. **C99**, 024313 (2019).
- [12] E. Epelbaum *et al.* [LENPIC Collaboration], arXiv:1907.03608 [nucl-th], *to be published in Eur. Phys. J. A.*
- [13] W. Glöckle *et al.*, Phys. Rep. **274**, 107 (1996).
- [14] N. Kalantar-Nayestanaki, E. Epelbaum, J. G. Messchendorp, and A. Nogga, Rep. Prog. Phys. **75**, 016301 (2012).
- [15] E. Stephan *et al.*, Phys. Rev. C **76**, 057001 (2007).
- [16] K.Sekiguchi *et al.*, Phys. Rev. **C79** (2009) 054008.
- [17] E.Stephan *et al.*, Eur. Phys. J. **A42** (2009) 13.
- [18] E.Stephan *et al.*, Phys. Rev. **C82** (2010) 014003.
- [19] I. Ciepał *et al.*, Phys. Rev. **C85** (2012) 017001.
- [20] K.Sekiguchi *et al.*, Phys. Rev. **C89** (2014) 064007.
- [21] K.Sekiguchi *et al.*, Phys. Rev. **C96** (2017) 064001.
- [22] H. Tavakoli-Zaniani *et al.*, arXiv:1908.10071 [nucl-ex].
- [23] M.Mohammadi-Dadkan *et al.*, arXiv:1910.13605 [nucl-ex].
- [24] J. Carlson, R. Schiavilla, Rev. Mod. Phys. **70**, 743 (1998).
- [25] S. Kölling, E. Epelbaum, H. Krebs and U.-G. Meißner, Phys. Rev. **C80**, 045502 (2009).
- [26] S. Kölling, E. Epelbaum, H. Krebs and U.-G. Meißner, Phys. Rev. **C84**, 054008 (2011).
- [27] H. Krebs, E. Epelbaum and U.-G. Meißner, Annals Phys.**378**, 317 (2017).
- [28] H. Krebs, E. Epelbaum and U.-G. Meißner, Few Body Syst. **60**, 31 (2019).
- [29] S. Pastore, R. Schiavilla and J. L. Goity, Phys. Rev. **C78**, 064002 (2008).
- [30] S. Pastore, L. Girlanda, R. Schiavilla, M. Viviani and R.B. Wiringa, Phys. Rev. **C80**, 034004 (2009).
- [31] T. Kii, T. Shima, T. Baba, and Y. Nagai, Nucl. Instrum. Methods **A552**, 329 (2005).
- [32] H. R. Weller, M. W. Ahmed, H. Gao, W. Tornow, Y. K.Wu, M. Gai, and R. Miskimen,Prog. Part. Nucl. Phys. **62** ,257 (2008).
- [33] K. Kramer, X. Zong, R. Lu, D. Dutta, H. Gao, X. Qian, Q. Ye, X. Zhu, T. Averett, and S. Fuchs, Nucl. Instrum. Methods Phys. Res., Sect. **A582**, 318 (2007).
- [34] A. Watanabe, S. Nakai, K. Sekiguchi et al., Recent Progress in Few-Body Physics, Springer, in press (the conference proceedings of FB22)

- [35] R. B. Wiringa *et al.*, Phys. Rev. C **51**, 38 (1995).
- [36] B. S. Pudliner *et al.*, Phys. Rev. C **56**, 1720 (1997).
- [37] J. Golak *et al.*, Phys. Rep. **415**, 89 (2005).
- [38] R. Skibiński, J. Golak, H. Witała, W. Glöckle, A. Nogga, Eur. Phys. J. **A24**, 31 (2005).
- [39] H. Arenhövel, arXiv:0804.2559v1 [nucl-th].
- [40] D. Hüber *et al.*, Acta Phys. Polonica B **28**, 1677 (1997).
- [41] W. Glöckle, The Quantum Mechanical Few-Body Problem, Springer-Verlag 1983.
- [42] A. Nogga, A. Kievsky, H. Kamada, W. Glöckle, L.E. Marcucci, S. Rosati, M. Viviani, Phys. Rev. C **67**, 034004 (2003).
- [43] H. Witała, W. Glöckle, Th. Cornelius, Phys. Rev. C **39**, 384 (1989).
- [44] H. Witała, W. Glöckle, H. Kamada, Phys. Rev. C **43**, 1619 (1991).
- [45] H. Witała and W. Glöckle, J. Phys. G: Nucl. Part. Phys. **37**, 064003 (2010).
- [46] G. Rauprich *et al.*, Nucl. Phys. **A535**, 313 (1991).
- [47] H. R. Setze *et al.*, Phys. Lett. **B388**, 229 (1996).
- [48] K. Sagara, Few-Body Systems **48**, 59 (2010).

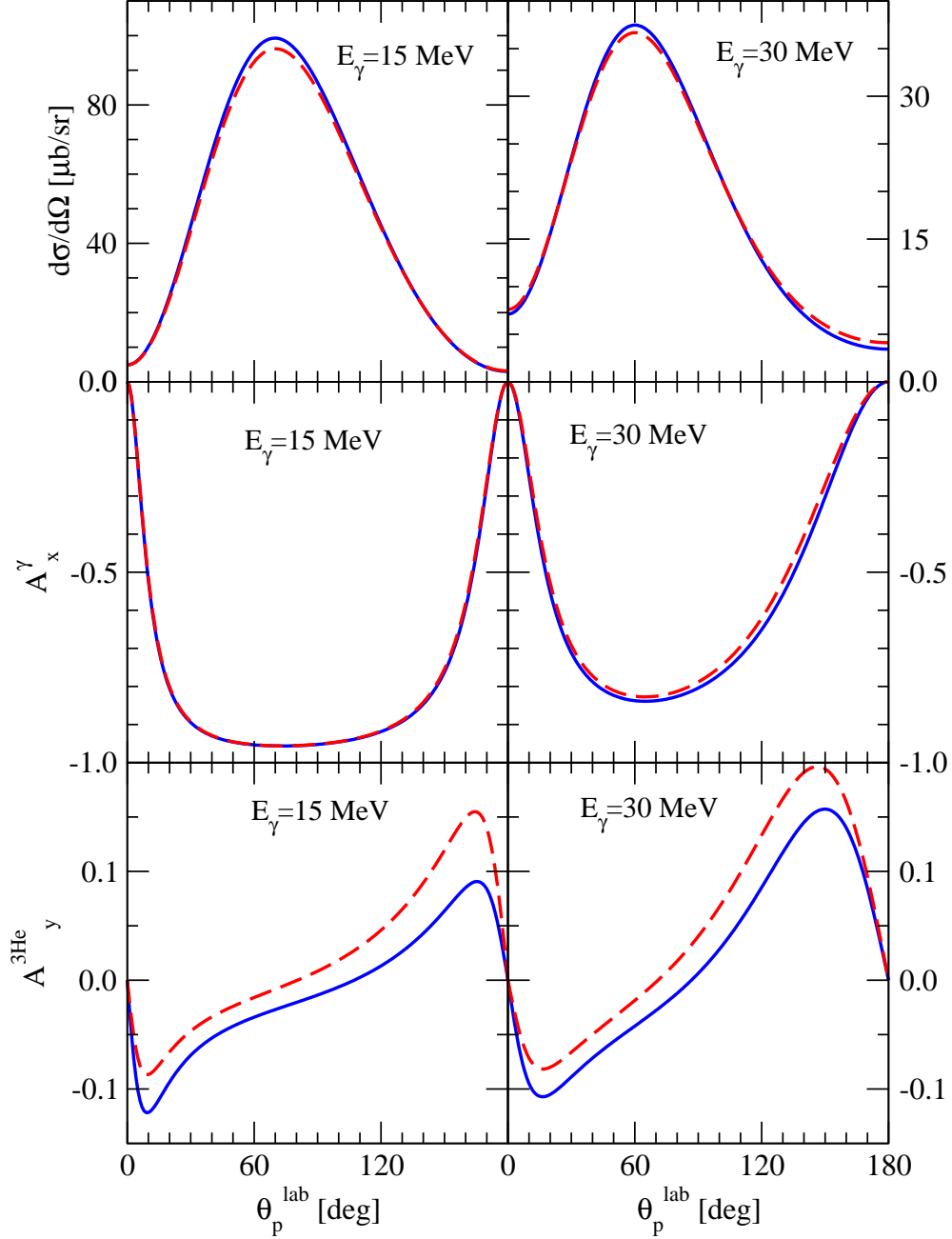


FIG. 1. (Color online) The unpolarized cross section and the analyzing powers: A_x^γ and A_y^{3He} , for two-body ${}^3\text{He}$ photodisintegration ${}^3\vec{H}e(\vec{\gamma}, p)d$ at $E_\gamma = 15$ MeV (left column) and $E_\gamma = 30$ MeV (right column). Presented results are based on AV18 NN interaction combined with Urbana IX 3NF, and ${}^3\text{He}$ current which, in addition to single nucleon current, contained two-body exchange contributions taken in the form of meson-exchange currents ((blue) solid line) or by Siegert theorem ((red) dashed line).

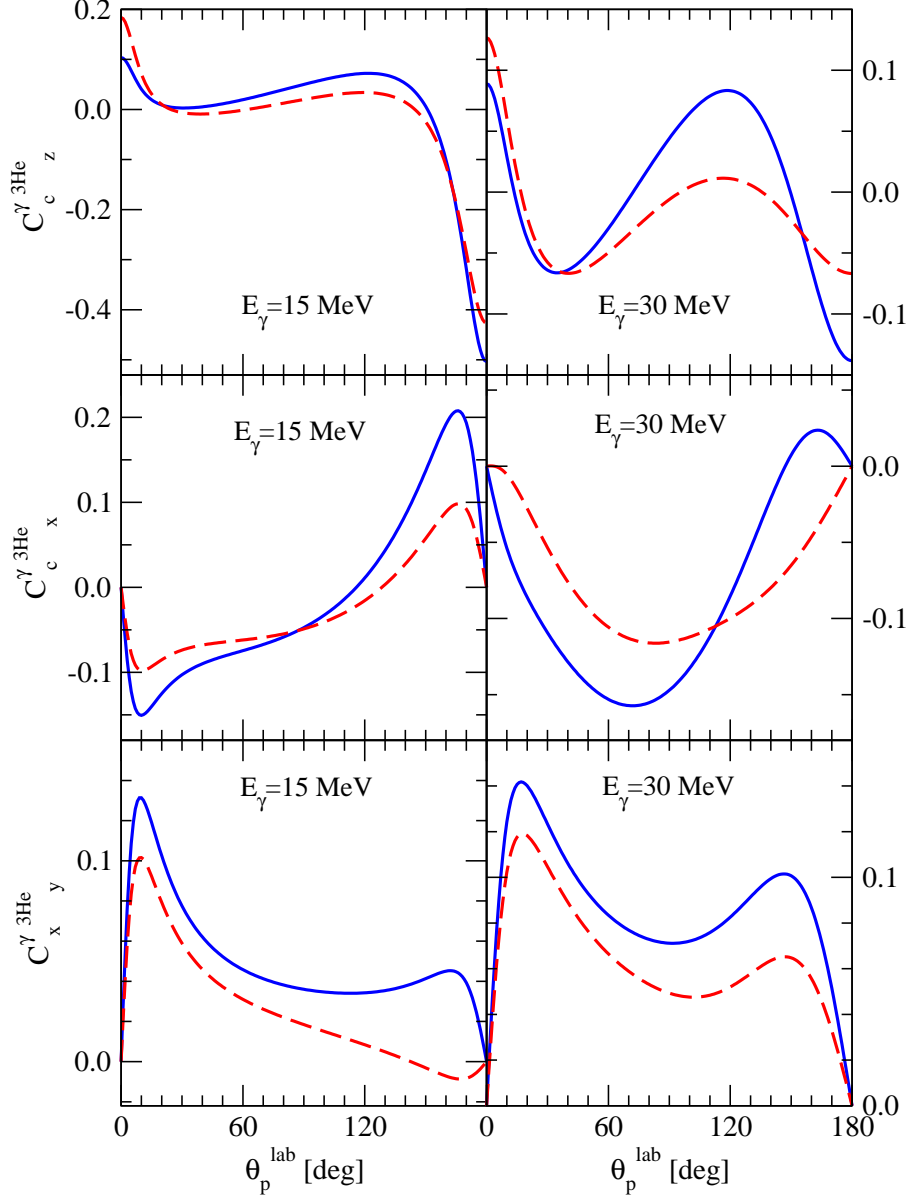


FIG. 2. (Color online) The spin correlation coefficients $C_{c-z}^{\gamma-3\text{He}}$, $C_{c-x}^{\gamma-3\text{He}}$, and $C_{x-y}^{\gamma-3\text{He}}$ for two-body ${}^3\text{He}$ photodisintegration ${}^3\vec{H}e(\vec{\gamma}, p)d$ at $E_\gamma = 15$ MeV (left column) and $E_\gamma = 30$ MeV (right column). Lines are the same as in Fig.1.

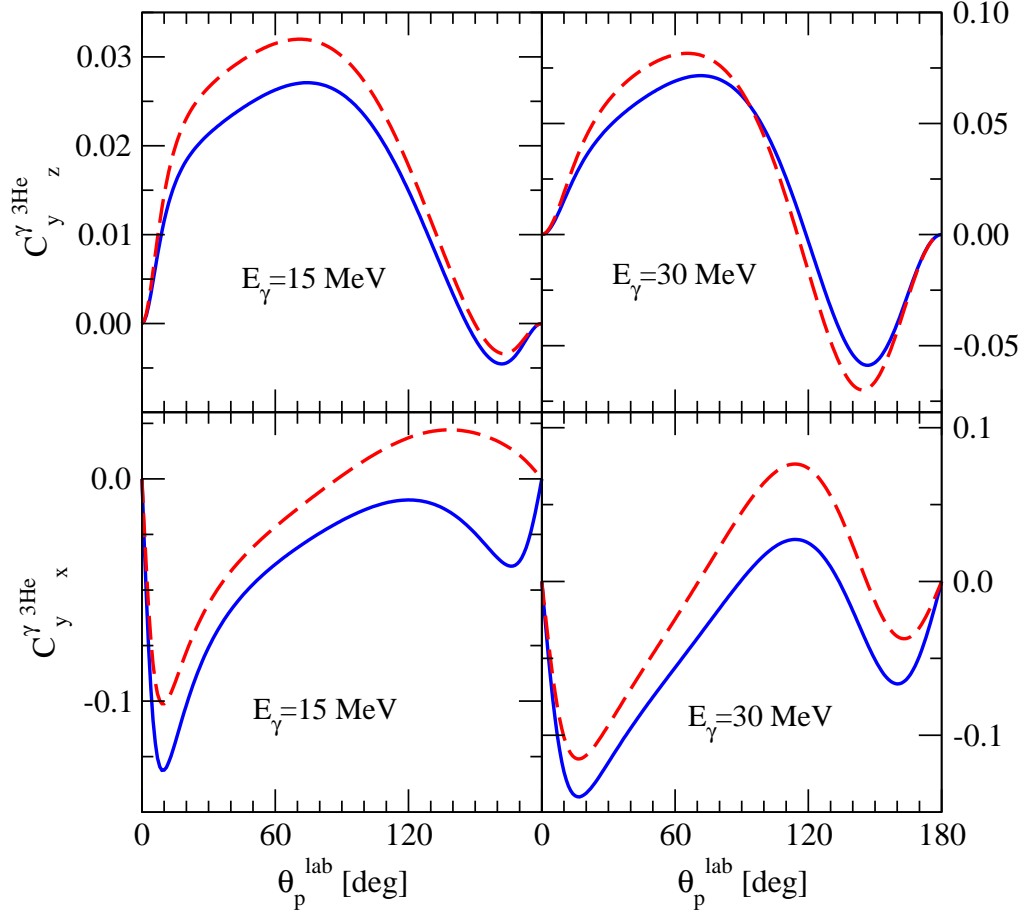


FIG. 3. (Color online) The spin correlation coefficients $C_{y z}^{\gamma 3He}$ and $C_{y x}^{\gamma 3He}$ for two-body ${}^3\text{He}$ photodisintegration ${}^3\vec{H}e(\vec{\gamma}, p)d$ at $E_{\gamma} = 15$ MeV (left column) and $E_{\gamma} = 30$ MeV (right column). Lines are the same as in Fig.1.

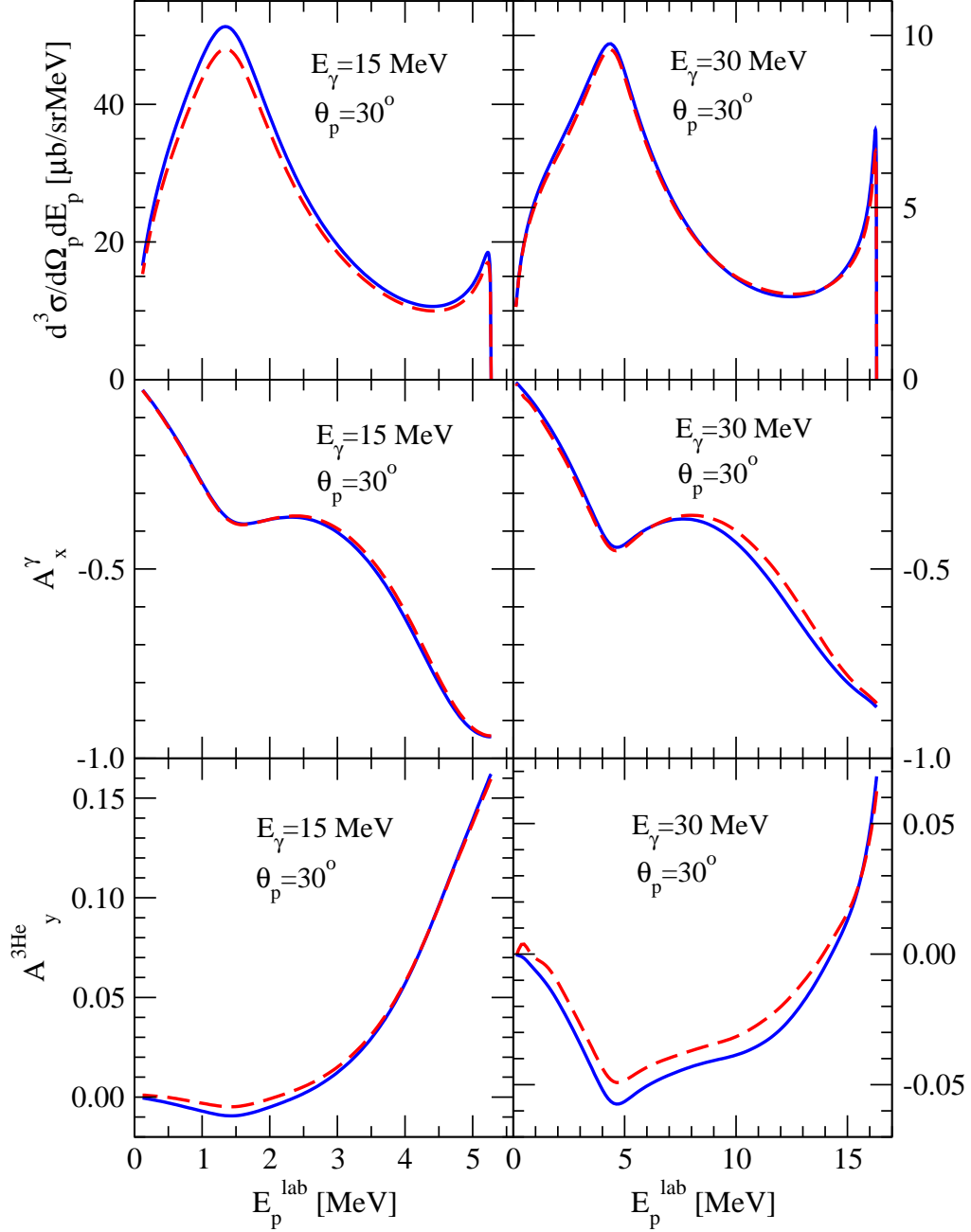


FIG. 4. (Color online) The unpolarized cross section and the analyzing powers: A_x^γ and A_y^{3He} , for semi-inclusive three-body ${}^3\text{He}$ photodisintegration ${}^3\vec{H}e(\vec{\gamma}, p)np$ at $E_\gamma = 15$ MeV (left column) and $E_\gamma = 30$ MeV (right column) as a function of the laboratory energy E_p^{lab} of the outgoing proton detected at lab. angle $\theta_p = 30^\circ$. Lines are the same as in Fig.1.

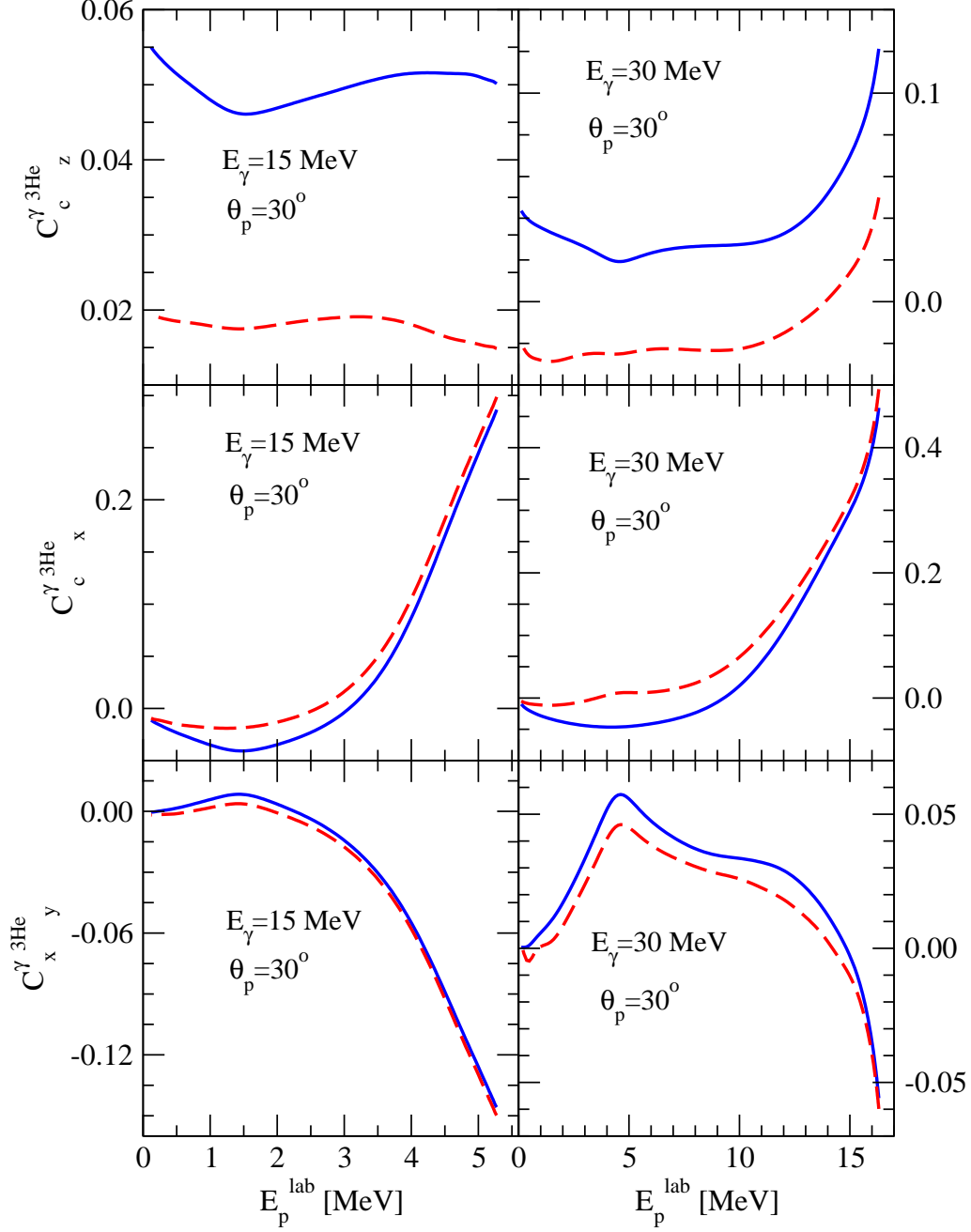


FIG. 5. (Color online) The same as in Fig.4 but for spin correlation coefficients $C_{c-z}^{\gamma-^3\text{He}}$, $C_{c-x}^{\gamma-^3\text{He}}$, and $C_{x-y}^{\gamma-^3\text{He}}$. Lines are the same as in Fig.1.

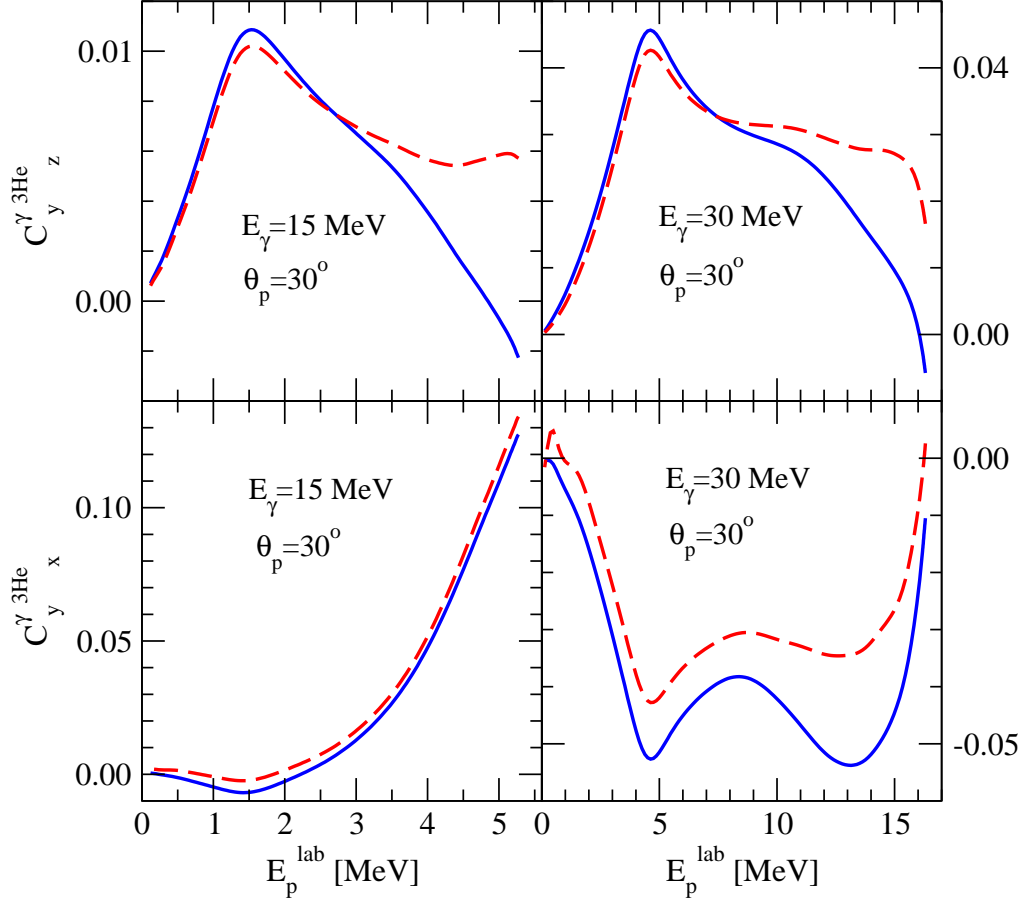


FIG. 6. (Color online) The same as in Fig.4 but for spin correlation coefficients $C_{y z}^{\gamma 3He}$ and $C_{y x}^{\gamma 3He}$. Lines are the same as in Fig.1.

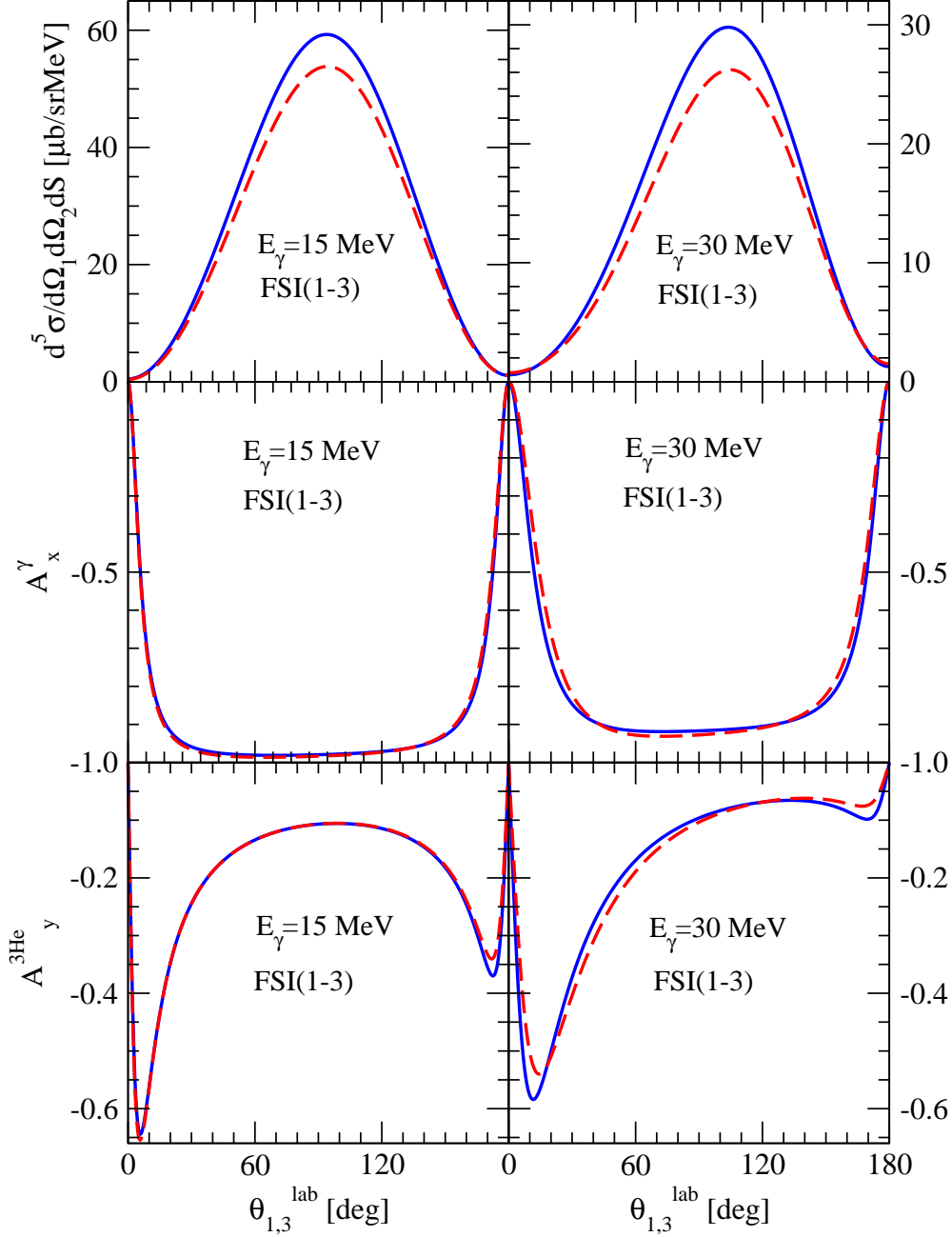


FIG. 7. (Color online) The unpolarized cross section $\frac{d^5\sigma}{d\Omega_1 d\Omega_2 dS}$ and the analyzing powers: A_x^γ and $A_y^{^3\text{He}}$, for exclusive three-body ^3He photodisintegration $^3\vec{H}e(\vec{\gamma}, pp)n$ at $E_\gamma = 15$ MeV (left column) and $E_\gamma = 30$ MeV (right column), for kinematically complete final state interaction configuration, where nucleons 1 and 3 (proton and neutron, respectively) have the same momenta $\vec{p}_1 = \vec{p}_3$. The observables are shown as a function of the laboratory angle $\theta_1^{lab} = \theta_3^{lab}$ at which that configuration is produced. Lines are the same as in Fig.1.

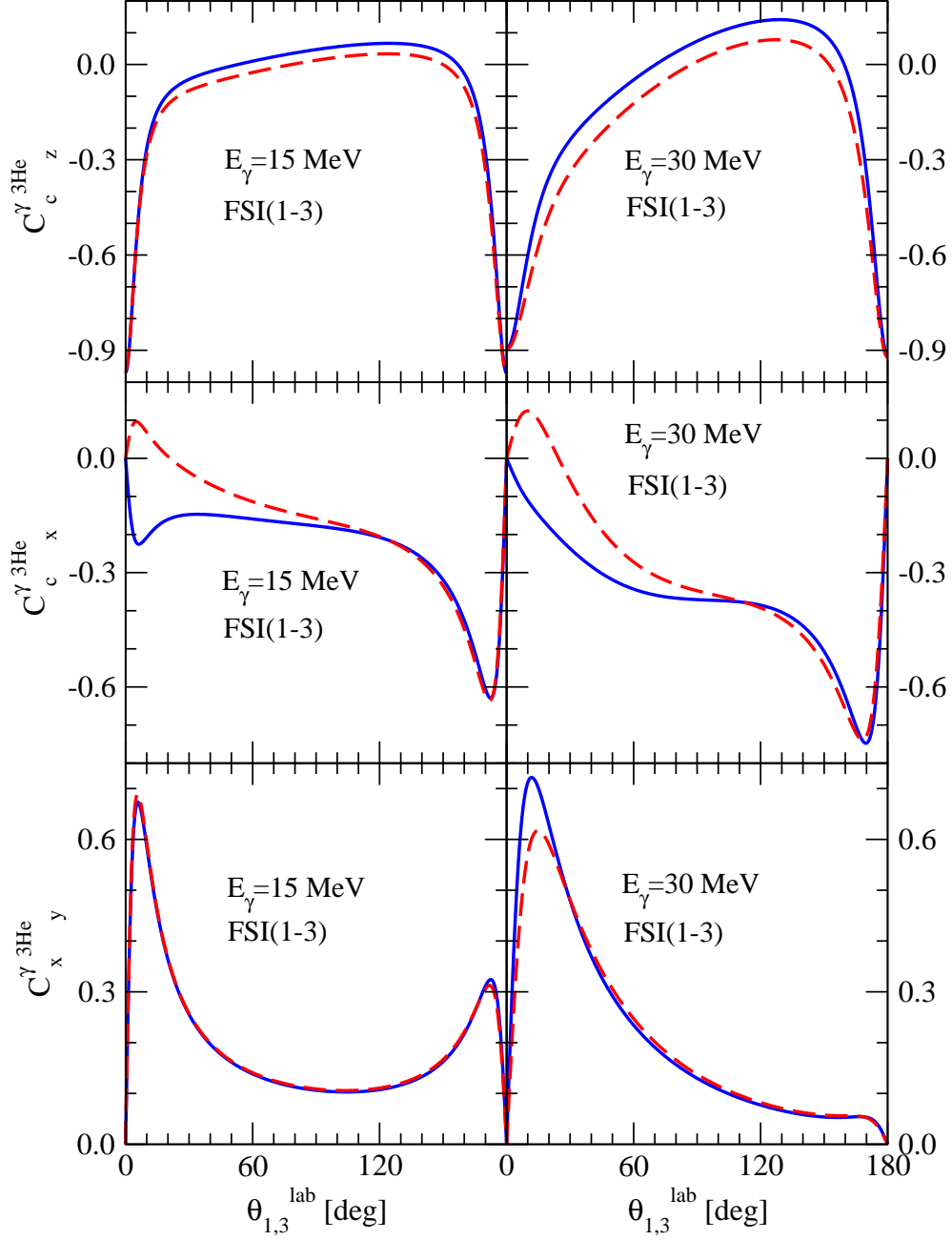


FIG. 8. (Color online) The same as in Fig.7 but for spin correlation coefficients $C_{c-z}^{\gamma-3\text{He}}$, $C_{c-x}^{\gamma-3\text{He}}$, and $C_{x-y}^{\gamma-3\text{He}}$. Lines are the same as in Fig.1.

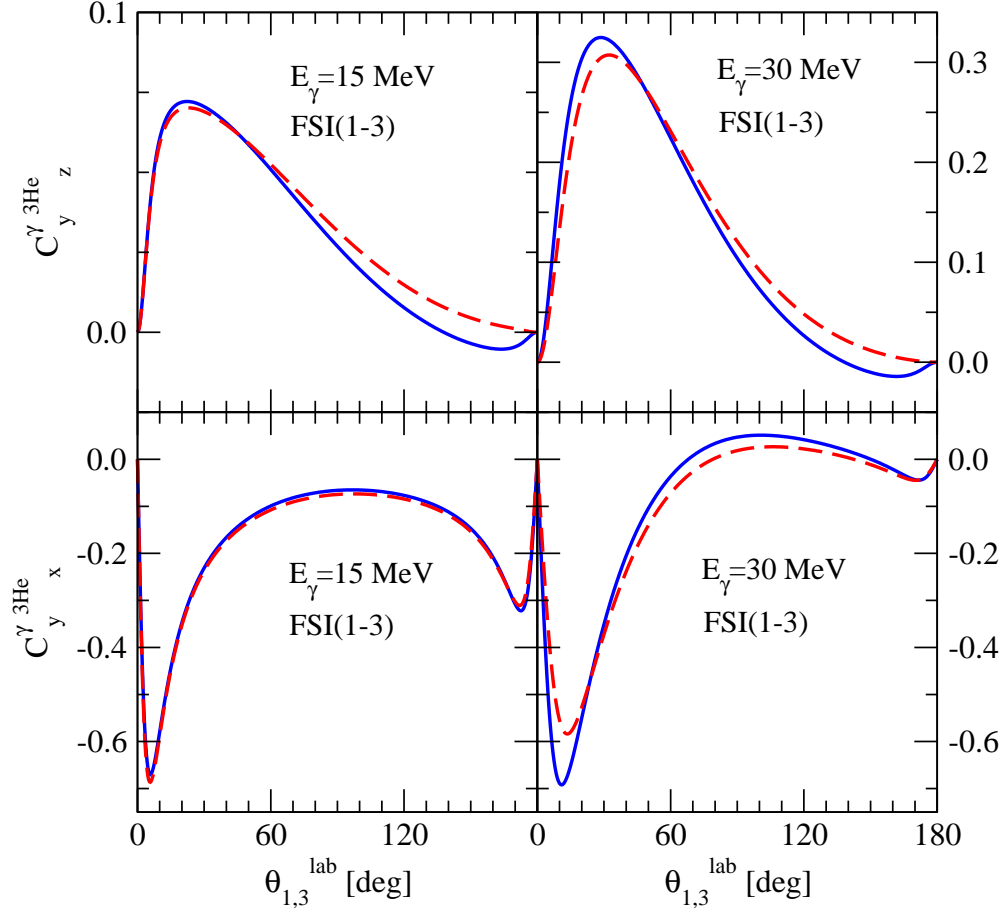


FIG. 9. (Color online) The same as in Fig.7 but for spin correlation coefficients $C_{y z}^{\gamma \text{ } ^3\text{He}}$ and $C_{y x}^{\gamma \text{ } ^3\text{He}}$.

Lines are the same as in Fig.1.

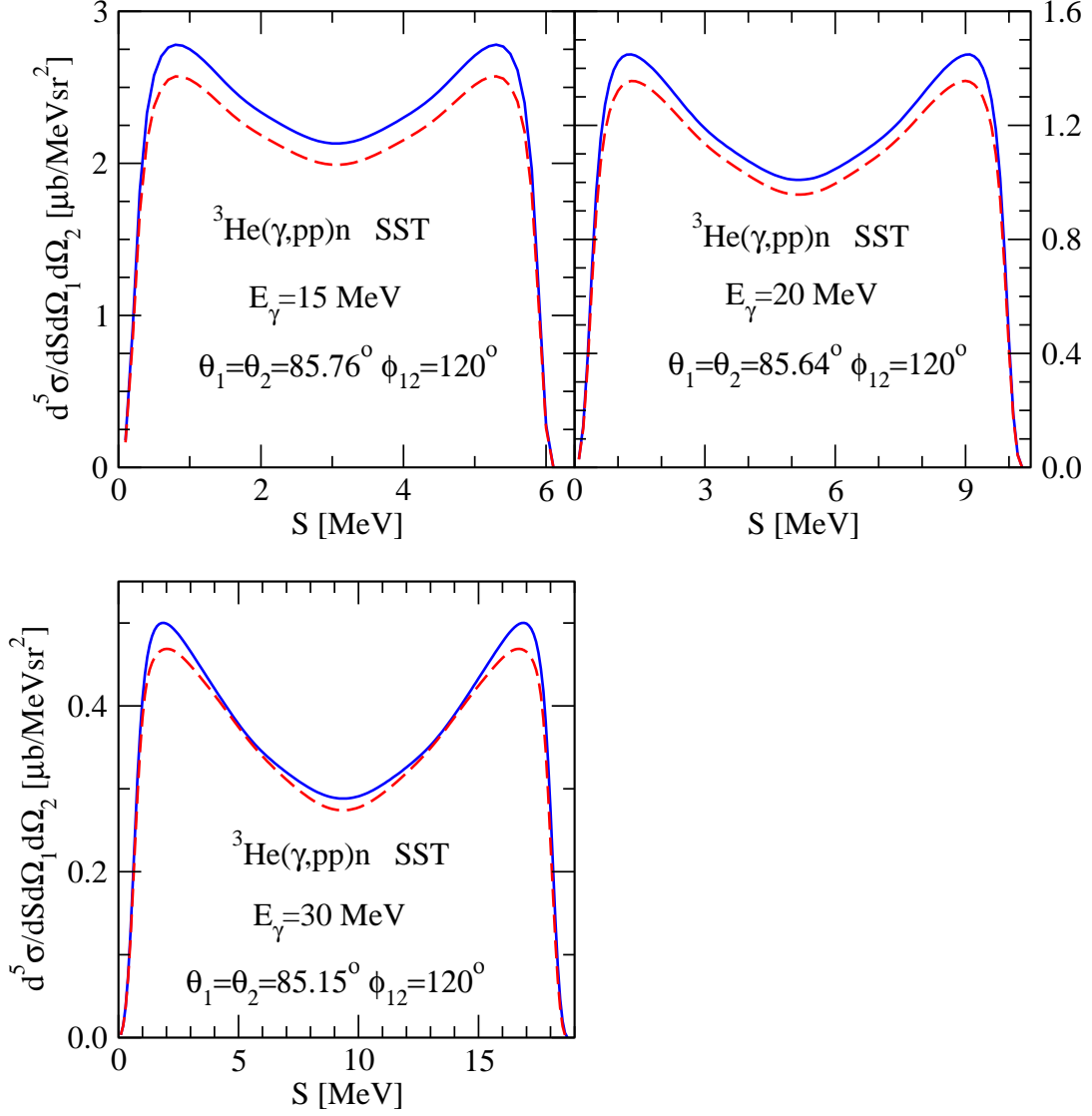


FIG. 10. (Color online) Unpolarized cross section for exclusive three-body ${}^3\text{He}$ photodisintegration ${}^3\vec{H}e(\vec{\gamma}, pp)n$ at $E_\gamma = 15, 20,$ and 30 MeV, in a kinematically complete space star geometry, shown as a function of arc-length of the S-curve in the plane of laboratory energies of nucleons 1 and 2. Lines are the same as in Fig.1.